Rare Metal Materials and Engineering
Volume 48, Issue 3, March 2019
Available online at www.rmme.ac.cn

Science Press

Cite this article as: Rare Metal Materials and Engineering, 2019, 48(3): 0728-0738.

ARTICLE

Effect of Vibration on Remanufacturing Microstructure of FV520B Stainless Steel Using MAG Surfacing Deposition Technology

Liu Jian[1], Zhu Sheng[2], Cai Zhihai[1], Zhang Ping[1], Liu Jun[1], Qin Hang[1], Tong Yonggang[1]

[1] *National Engineering Research Center for Mechanical Product Remanufacturing, Academy of Armored Forces Engineering, Beijing 100072, China*; [2] *National Defense Key Laboratory for Remanufacturing Technology, Academy of Armored Force Engineering, Beijing 100072, China*

Abstract: The remanufacturing experiment of FV520B precipitation hardening stainless steel was carried out by metal active gas arc welding (MAG) surfacing deposition technology. On this basis, the characteristics of remanufacturing microstructure were analyzed, and the effect of mechanical vibration on remanufacturing microstructure was studied. The results show that the remanufacturing microstructure of FV520B stainless steel by MAG surfacing deposition technology is composed of martensite+carbide precipitation-hardening phase. It exhibits a characteristic of periodical variation along the direction of forming height, which is described by certain self-similar fractal characteristics. The vibration increases the probability of twin formation to some extent, which has a broken effect on the martensite lath. The width of the martensite lath decreases first and then increases with the continuous increase of the vibration rotation rate. Affected by the vibration, the lattice distortion and the preferred orientation (TC) of each crystal plane are changed. However, the change rule of different crystal planes is different. The Bragg diffraction peak positions of planes (110) and (211) shift toward the direction of lower diffraction angle due to the addition of vibration. Furthermore, the offset increases first and then decreases with the continuous increase of the vibration speed. Meanwhile, the FWHM of diffraction peak (110) decreases first and then increases while the preferred orientation of this crystal plane increases first and then decreases. Within the range between 0 and the resonance speed, the FWHM of diffraction peak (211) decreases first and then increases with the continuous increase of the vibration speed, and then decreases again when the vibration speed is higher than the resonance speed. However, its TC continues to increase with the increase of the vibration rotation rate. In general, the sub-resonance frequency (the vibration rotational speed f=3000 r/min) has the most significant effect on the remanufacturing microstructure of FV520B stainless steel using MAG surfacing deposition technology.

Key words: FV520B precipitation hardening stainless steel; remanufacturing; MAG surfacing; vibration; microstructure

FV520B stainless steel is a kind of martensitic precipitation-hardening stainless steel, with the advantages of high strength, good weldability and easy processing etc. It is mainly used for manufacturing medium-high-speed wind turbine blades with some abrasive particles and corrosive medium[1-4].

Although FV520B stainless steel has excellent properties, its price is very high. Meanwhile, the blade has very short lifetime and is easy to reach the failure point under harsh working conditions. So, it has important economic signifi-

Received date: March 9, 2018
Foundation item: National Natural Science Foundation of China (51405510, 51375492, 51575527)
Corresponding author: Zhu Sheng, Professor, National Defense Key Laboratory for Remanufacturing Technology, Academy of Armored Force Engineering, Beijing 100072, P. R. China, Tel: 0086-10-66717206, E-mail: zusg@sohu.com

cance and academic value to research the remanufacturing of failure components of FV520B stainless steel. At present, there is few relevant research that has been carried out abroad on FV520B stainless steel [5]. Domestic in-depth studies have been carried out on the machinability of FV520B stainless steel [6-8], stainless steel heat treatment technology and property [9-12], FV520B stainless steel welding [13-17] and surface hardening of this steel [18,19]. The research basis behind remanufacturing components of FV520B stainless steel is, however, still relatively weak. Only a few studies on remanufacturing of FV520B stainless steel by the laser cladding forming (LCF) technology have been reported [2,20]. Research on remanufacturing of FV520B stainless steel by surfacing deposition technology has been seldom reported. In contrast, active gas arc welding (MAG) surfacing deposition technology has the advantages of high efficiency, high material utilization rate and low cost etc. Therefore, this paper mainly studied the characteristics of remanufacturing microstructure and the effect of mechanical vibration on FV520B stainless steel by adopting the MAG surfacing deposition technology. It lays the foundation for clarifying the remanufacturing characteristics of FV520B stainless steel by MAG surfacing deposition technology and further develops high-quality and high-efficiency parts of FV520B stainless steel.

1 Experiment

The substrate FV520B stainless steel material is manufactured by Beiman Special Steel Company Limited, with the size of 120 mm×65 mm×6 mm. The remanufacturing and forming material corresponds to the special solid core welding wire of FV520B stainless steel characterized by a diameter of 1.2 mm. The chemical composition of the solid core wire and substrate is shown in Table 1. The protective gas used for the experiment is a mixed gas containing 98% Ar and 2% O_2. The room temperature is 20 °C. Meanwhile, the vibration system is a HK-93 microcomputer vibrating stress relief device made by Hua Yun Mechanical & Electric Science and Technology Company Limited. The size of the vibration platform is 2000 mm×500 mm×20 mm, and the material is 45 steel.

Before starting the experiment, the remanufacturing substrate and vibration machine were separately fastened on positions which were relatively close to the middle of the platform. During the experiment, the process parameters are as follows: a wire feed speed of 8.8 m/min, a surfacing speed of 21 mm/s, a welding torch space of 13 mm, an arc length correction of 30% and a gas flow of 21 L/h. The path pattern in a specific layer was a Chinese character "弓" shaped path and the path pattern between the layers was mutually orthogonal, referred to the Ref.[21]. The remanufacturing size was 100 mm × 65 mm × 100 mm. When loading a vibration to implement the experiment, the vibration speeds were f=1500, 3000, 5000, 8000 r/min. Among these, the vibration speed of f=5000 r/min corresponded to the resonance speed between the vibration machine and the platform which was measured in the previous experiments. After the experiment, the remanufacturing microstructure of FV520B stainless steel by MAG surfacing deposition technology under different conditions was observed and analyzed by instruments such as optical microscope (OM, model number: OLYMPUS-DP12), scanning electron microscope (SEM, model number: Quanta 200), transmission electron microscope (TEM, model number: JEOL-2100), energy disperse spectroscopy (EDS, model number: X-Max80) and X-ray diffractometer (XRD, model number: D8 Advance). Afterwards, the effect of vibration on remanufacturing microstructure of FV520B stainless steel by MAG surfacing deposition technology was studied.

The etching solution composition of the metallographic specimen was a mixed solution of 5 mL hydrochloric acid and 1 g picric acid, as well as 100 mL ethyl alcohol. The etching time was 20~30 s (at room temperature). In addition, the transmission electron microscope (TEM) specimen was prepared using the ion-thinning method.

2 Results and Discussion

2.1 Remanufacturing microstructure

Fig. 1 shows the remanufacturing metallographic microstructure image of FV520B stainless steel by MAG surfacing deposition technology. It can be deduced from the analysis that the remanufacturing microstructure is comprised of lath martensite and carbide precipitated at grain boundaries and inside the grains. Fig. 2 displays the XRD analysis of the remanufacturing layer of FV520B stainless steel by MAG surfacing deposition technology. It can be seen from the figure that the XRD diffraction peak is a complete martensitic diffraction peak. This illustrates that the matrix microstructure of the remanufacturing layer is mainly the martensite.

Fig. 3 illustrates the TEM micrograph of the remanufacturing microstructure. It can be seen from the images that the martensitic lath bundles are clearly visible and orderly arrayed. This leads to the conclusion that the crystal growth direction of the remanufacturing layer has a relatively apparent preferred orientation. Meanwhile, it can also be seen from the images that the dislocation density in the martensitic lath is high and that the phenomenon of dislocation tangle is apparent.

Fig. 3b corresponds to the partially segregated precipitation image of the precipitated hardening phase in the remanufacturing layer. The results of the energy spectrum show that the Nb element in the precipitated phase is highly enriched, which indicates that the enriched and precipitated hardening phase is NbC. The segregation of the carbide reinforcement phase has harmful effects on the precipitation

Table 1 Chemical composition of remanufacturing wire and FV520B stainless steel (wt%)

Element	C	Mn	Si	S	P	Cr	Ni	Cu	Mo	Nb	Fe
Base metal	0.062	0.67	0.44	0.005	0.026	13.37	5.33	1.46	1.44	0.29	Bal.
Wire	0.033	0.55	0.35	0.011	0.017	14.2	6.42	-	1.17	0.33	Bal.

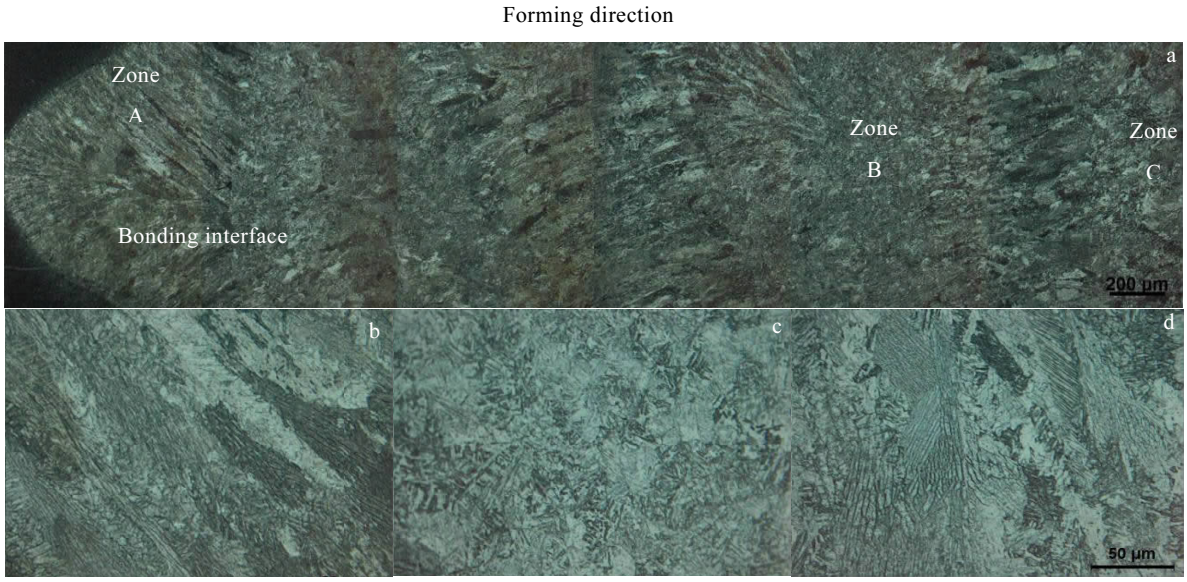

Fig.1 Remanufacturing microstructures of different regions of FV520B stainless steel using MAG surfacing deposition technology: (a) microstructure variation along the forming height direction, (b) co-genetic columnar crystals of interface in zone A, (c) fine grained region between layers in zone B, and (d) columnar crystals of the surface layer in zone C

strengthening effect of dispersed precipitation on the substrate.

It can also be seen from Fig. 1a that in the metallographic microstructure along the forming height direction, a feature of layered periodical variation obviously appears. It can generally be classified into the interlayer bonding zone (including the bonding zone between the forming layer and the substrate), interior zone of the forming layer and the surface zone. The microstructures of different zones are clearly different. The microstructure in the bonding zone between the forming layer and the substrate can be characterized by obvious columnar crystals which are developed perpendicular to the tangential direction of the bonding interface contour (the microstructure of zone A in Fig. 1a). The grains are fine. The growth direction of the grains in the interior of the forming layer is disordered and the martensite lath is relatively large. This corresponds to the microstructure of zone B in Fig. 1a. The columnar crystals in the surface zone of the forming layer (the microstructure of zone C in Fig. 1a) are relatively obvious as well. However they are not as regular as zone A and the grains are larger.

Furthermore, the remanufacturing is completed layer by layer and the forming process of each layer is similar. Even the microstructure of each layer is similar. Consequently, it can be said that the remanufacturing microstructure of

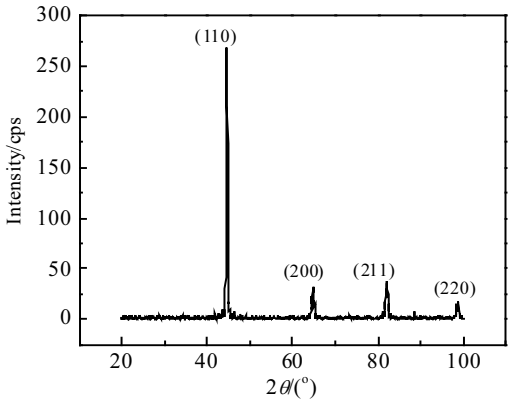

Fig. 2 X-ray diffraction pattern of remanufacturing layer

FV520B stainless steel by MAG surfacing deposition technology has the self-similar characteristic to a certain extent. Adopting the digital image method, the fractal dimensions of Fig. 1b and 1c are calculated as 2.5347 and 2.561, respectively. According to the research results of Ref.[22, 23], the larger the fractal dimension, the more complex the surface microstructure of the research object. It coincides with the fact that the array of the microstructure in the central

zone of the forming layer exists in a disordered manner and is unsystematic without any apparent regularity. Therefore, it can be said that the remanufacturing microstructure of FV520B stainless steel by MAG surfacing deposition technology corresponds to a fractal body within a certain range.

2.2 Effect of vibration on remanufacturing microstructure

2.2.1 Effect of vibration on remanufacturing microstructure

Fig.4 corresponds to a partial TEM image of the forming layer at *f*=8000 r/min. It can be clearly seen from the image that we have developed a fragment of martensite laths. This indicates that the incorporation of vibration leads to a broken effect on the remanufacturing martensite laths.

Fig.5 illustrates the TEM images of the remanufacturing interior zones (zone A shown in Fig.1) under the conditions of four different vibration speeds. Through the application of the measuring calculation, when the rotation speeds are *f*=1500, 3000, 5000 and 8000 r/min, the widths of martensite laths are 0.26, 0.21, 0.26 and 0.48 μm, respectively. Compared with Fig.3a (the width of martensite lath is about 0.27 μm), it can be seen that after a vibration is added in the remanufacturing process, the widths of the martensite laths narrow at first and then widen with the increase of vibration speed. The refining effect of vibration is the strongest at the sub-resonance rotation speed of *f*=3000 r/min with consequences on the width of martensite lath.

In addition, when the vibration rotation speed *f*=8000 r/min is used, observations of the remanufacturing microstructure show that there is a twinning, as shown in Fig.6. It shows that the generation probability of twin crystals may be increased after the addition of vibration.

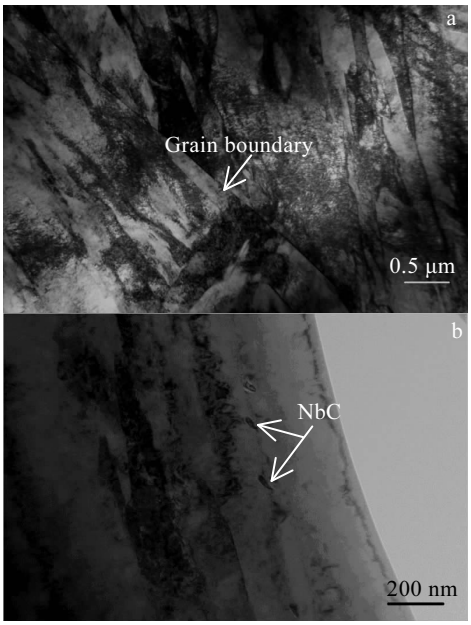

Fig.3 TEM images of remanufacturing layer: (a) martensite lath and (b) precipitated hardening phase

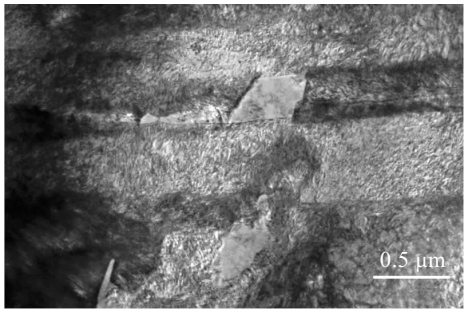

Fig.4 TEM image of lath martensite fragments

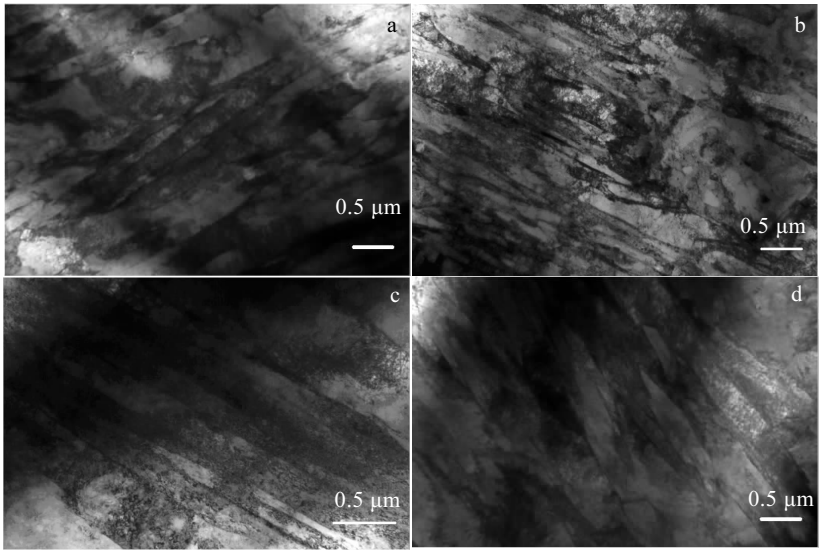

Fig.5 TEM images of lath martensite under different vibration speeds: (a) *f*=1500 r/min, (b) *f*=3000 r/min, (c) *f*=5000 r/min, and (d) *f*=8000 r/min

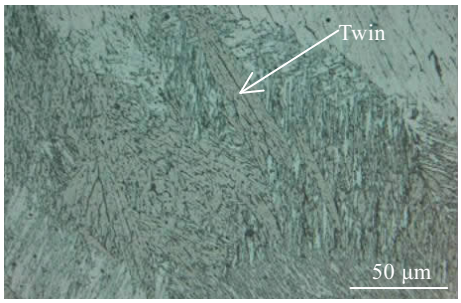

Fig.6 Twin crystals in the remanufacturing layer under the condition of vibration

2.2.2 Effect of vibration on the crystal lattice

Fig.7 shows the results of the XRD diffraction measurements of the remanufacturing layer of FV520B stainless steel by MAG surfacing deposition technology under the conditions of different vibration speeds. Compared with Fig.2, it can be clearly seen that the intensity and width of the diffraction peak of the remanufacturing layer change significantly after a vibration is applied. Furthermore, contrastive analyses are carried out on the Bragg diffraction peaks and the FWHMs of crystal planes (110) and (211) under the conditions of different vibration rotation speeds. The comparison results of diffraction peaks are shown in Fig. 8, and the FWHMs of crystal planes are shown in Table 2, where f=0 means that no vibration is applied during the remanufacturing process. It can be seen from Fig.8 that the diffraction peak positions of crystal planes (110) and (211) have roughly the same variation trends when applying mechanical vibration. When f≤3000 r/min, the diffraction peak position of the crystal plane shifts to the direction of the low diffraction angle, and the offset increases with the increase of the vibration rotation speed. When f=3000 r/min, the offset is the maximum. After that, the offset decreases with the continuous increase of the vibration rotation speed. When the vibration speed increases to f=8000 r/min, the diffraction peak position is hardly offset, in comparison with the non-vibration state.

The data in Table 2 show that the addition of vibration reduces the FWHMs of the diffraction peaks, namely which are narrowed, of crystal planes (110) and (211) to different extents. For crystal plane (110), when the vibration speed f≤3000 r/min, the FWHM of the diffraction peak performs a monotonic decreasing trend with the constant increase of the vibration speed, and reaches the minimum value when f=3000 r/min. However, with a further increase of the vibration speed, the FWHM of the diffraction peak increases slowly. This is highly consistent with the effect law of vibration on its diffraction peak position. In contrast, when the vibration speed f is within the interval of 0 r/min to

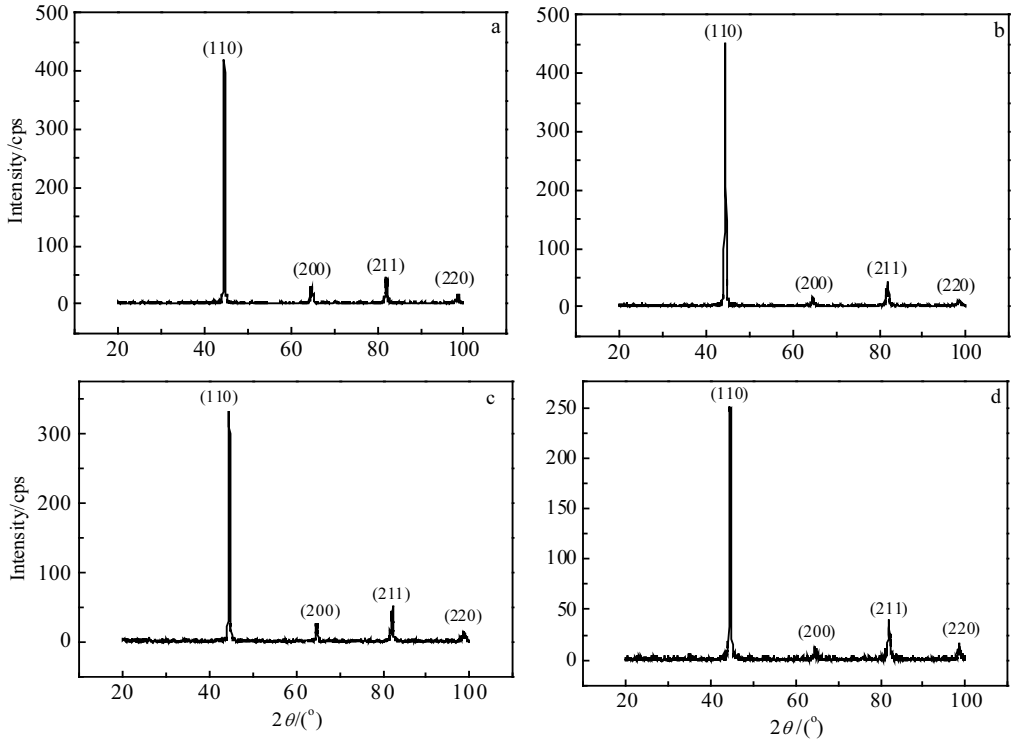

Fig.7 XRD patterns of remanufacturing formation layers under different vibration speed conditions: (a) f=1500 r/min, (b) f=3000 r/min, (c) f=5000 r/min, and (d) f=8000 r/min

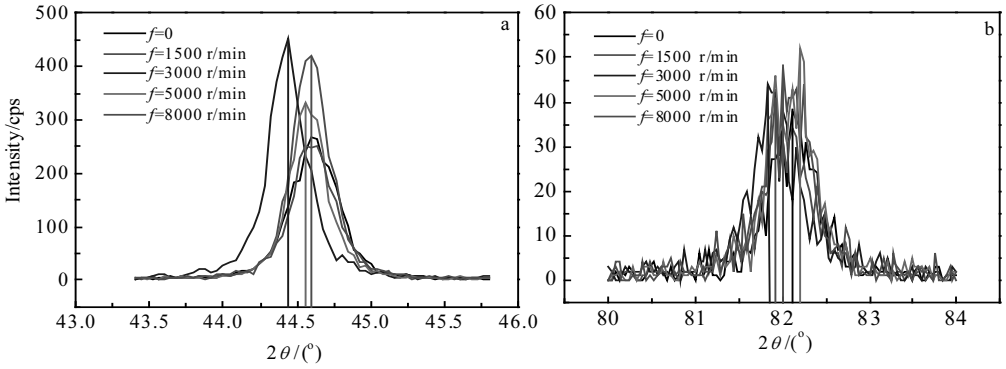

Fig. 8 Effects of vibration speed on Bragg scattering peak of lattice plane (110) (a) and lattice plane (211) (b)

Table 2 FWHM of Bragg diffraction peak of each crystal plane under the conditions of different vibration speeds

(*hkl*)	*f*=0 r/min	*f*=1500 r/min	*f*=3000 r/min	*f*=5000 r/min	*f*=8000 r/min
(110)	0.379º	0.322º	0.282º	0.286º	0.330º
(200)	0.605º	0.726º	0.480º	0.593º	0.262º

5000 r/min, the performance of crystal plane (211) in the diffraction peak FWHM is the same as that of crystal plane (110). However, when $f>5000$ r/min, the FWHM of the diffraction peak quickly gets reduced, even lower than at *f*=3000 r/min. This indicates that the effects of vibration on the different crystal planes are also different.

According to the X-ray diffraction theory, the linear variation of the Bragg diffraction peak is the combined result of the polycrystalline grain size variation, the lattice distortion variation and the widening of the instrument[24]. Since the widening of the instrument has the same effect on different specimens, it can therefore be dismissed. In this case, the linear narrowing of the diffraction peak is mainly caused by the variations of grain size and lattice distortion. Both the grain refinement and lattice distortion increase will cause a FWHM widening of the diffraction peak. The researches of Ref. [25-27] show that the vibration has an effect on grain refinement. This indicates that the addition of mechanical vibration can relieve the lattice distortion during the process of crystal formation. Also it implies that the vibration can relieve and even eliminate the stress in material. This is consistent with the numerous research conclusions that have been derived about vibration aging. Meanwhile, the linear narrowing effects of the Bragg diffraction peak caused by the vibrations with different rotation speeds are different. It shows that the vibrations of different rotation speeds have different effects on eliminating the lattice distortion.

2.2.3 Effect of vibration on crystal orientation

The diffraction peak intensity reflects the crystallographic orientation of materials. By comparing Fig.7 with Fig. 2, it can be obviously seen that the diffraction peak intensity of crystal plane (110) has a certain variation after a mechanical vibration is applied during the remanufacturing process. Even it illustrates that the remanufacturing crystallographic orientation of FV520B stainless steel using MAG surfacing deposition technology has changed correspondingly.

The highest intensity value of the diffraction peak is recorded as 100 unit intensity. The normalization processing of other diffraction peak intensities is carried out accordingly. The obtained values are recorded as I_m and compared with the diffraction intensity I_o which is calibrated by the standard ASTM card. According to Eq.(1) [28, 29], a preferred orientation factor (TC) is calculated and the effect of vibration on the crystallographic orientation of the remanufacturing layer is studied. The calculated results are shown in Table 3.

$$TC_{(hkl)j} = \frac{(I(hkl)j / I(hkl)j, 0)}{(1/n)\sum_{i=1}^{n}(I(hkl)i / I(hkl)i, 0)} \quad (1)$$

where I and I_0 are the experimental value and card value of (*hkl*) crystal plane's diffraction intensity, respectively, and n is the quantity of diffraction peaks studied in the experiment.

Comparing the data in Table 3, we can see that the application of vibration during the remanufacturing process changes the preferred orientation (TC) of each crystal plane, and the change laws of different crystal planes are different. Whether the vibration is imposed or not, the preferred orientation factor of crystal plane (110) is the maximum one among the four crystal planes, and is much larger than that of other crystal planes. It shows that crystal growth takes

place along a very strong preferred orientation during the remanufacturing process of FV520B stainless steel using MAG surfacing deposition technology, and the orientation of crystal plane (110) is the primary growth direction of crystals. After a vibration is imposed, the preferred orientation factor of crystal plane (110) increases first and then decreases with the constant increase of the vibration speed, but is always larger than the preferred orientation factor under the condition of no vibration applying. This indicates that the preferred orientation of crystal plane (110) increases first and then weakens with the constant increase of the vibration speed. And the application of vibration aggravates the growth behavior of crystal's preferred orientation during the remanufacturing process. When f=3000 r/min, the preferred orientation factor of crystal plane (110) is the maximum, which indicates that it has the greatest effect on the growth behavior of the crystal's preferred orientation.

The preferred orientation factor of crystal plane (220) decreases first and then increases with the constant increase of the vibration speed. When f=3000 r/min, the minimum value of 0.548 is recorded. At the vibration speed of f=8000 r/min, it is 1.083, which is larger than the value of 0.994 obtained under the condition of no vibration applying. This indicates that an imposed vibration with the rotation speed less than 8000 r/min weakens the preferred orientation of crystal plane (220). After a vibration is applied during the remanufacturing process, the preferred orientation factor values of crystal plane (211) are all larger than that obtained without any imposed vibration, and appear as a monotonous increasing trend. This indicates that the vibration increases the preferred orientation of this crystal plane during the remanufacturing process. Moreover, the higher the vibration speed, the stronger the preferred orientation. In contrast, the preferred orientation factor of crystal plane (200) generally exhibits a constant decreasing trend with the implementation of vibration. This suggests that its preferred orientation generally appears as a continuous decreasing trend with the constant increase of the vibration speed. The decreasing trend rises again only under the condition of resonance and drastically weakens soon after that.

Table 3 Crystal preferred orientation (TC) of the surface layer in the remanufacturing cross section of FV520B stainless steel using MAG surfacing deposition technology under the conditions of different vibration speeds

f/r·min^{-1}	(hkl)	I_m	I_o	$TC_{(hkl)}$
0	(110)	100	100	1.479
	(200)	11.194	20	0.828
	(211)	14.179	30	0.699
	(220)	6.716	10	0.994
1500	(110)	100	100	1.854
	(200)	6.921	20	0.642
	(211)	11.456	30	0.708
	(220)	4.296	10	0.796
3000	(110)	100	100	2.248
	(200)	4.213	20	0.473
	(211)	9.756	30	0.731
	(220)	2.439	10	0.548
5000	(110)	100	100	1.683
	(200)	8.108	20	0.682
	(211)	15.616	30	0.876
	(220)	4.505	10	0.758
8000	(110)	100	100	1.6
	(200)	5.578	20	0.446
	(211)	16.335	30	0.871
	(220)	6.773	10	1.083

2.3 Discussions

The solidification forming of surfacing material during the remanufacturing of FV520B stainless steel by MAG surfacing deposition technology is a rapid cooling non-equilibrium crystallization process. As a result, the martensite supersaturated solid solution microstructure is formed. Furthermore, a large number of dislocation defects exist in the martensite lath produced from the non-equilibrium crystallization. Meanwhile, since the cooling rate is too fast in the non-equilibrium crystallization process, the diffusion of precipitated solid-state atoms will be inhomogeneous and anon-equilibrium crystallization segregation will be caused, as shown in Fig.3b.

From the point of view of the fractal theory, the shaping process of the remanufacturing of FV520B stainless steel using MAG surfacing deposition technology is a "point-line-plane-body" developing process: the weld bead is formed with deposition molten drops, and each forming layer is built with weld beads arranged in accordance with certain rule. The forming layers stack one by one to complete the remanufacturing process at last. In addition, all the molten drops, weld beads and forming layers are self-similar. So it can be said that the remanufacturing process of FV520B stainless steel using MAG surfacing deposition technology has the characteristics of self-similar and periodic change. Therefore, the remanufacturing microstructure has the self-similar and periodic change characteristics that correspond to a fractal body within a certain scale range.

Furthermore, during the remanufacturing process, the heat dissipation in different zones is different, which induces the different crystallization behaviors in different zones. As a result, the microstructures in different zones are not the same. When the solidification of the molten pool in the first layer is started under the strong cooling effect of the substrate metal, an epitaxial solidification behavior occurs when the metal in the molten pool is solidified. The growth direction of grains is opposite to the thermal flow direction. Thus, the microstructure of the columnar crystal is formed perpendicular to the tangential direction of the molten pool contour. Furthermore, since remanufacturing has just started, the accumulation of thermal input is minor. Namely, the heat of the molten pool can be dissipated via the cold substrate, so the crystal grains are fine. In the interior of the molten pool, namely the central zone of the forming layer, the array of the martensite lath is disordered and unsystematic, without any obvious regularity, since the thermal dissipation is relatively slow and the thermal dissipation conditions along every direction are similar. Furthermore, the growing probabilities of grains along each direction after the nucleation are equal. In addition, the neighboring forming layer will have an effect of heat treatment on the adjacent formed layer. Influenced by this, a re-dissolving dispersive precipitation of the carbide reinforcement phase may occur. Therefore, its uniformity is relatively good even though the array of its microstructure is disordered.

In the constant process of remanufacturing, the above-mentioned solidification and crystallization behaviors are constantly recurring. However, the accumulation of thermal input continuously increases so that the microstructure of the corresponding location in the follow-up forming layer is relatively coarser. During the formation of the last layer, although a slower thermal dissipation is caused due to the accumulation of thermal input, the thermal flow directionality in its surface layer is relatively obvious. Some grains growing along the thermal-flow-reverse direction will slowly swallow up the grains growing along other directions and form a microstructure of columnar crystals which are relatively coarse. Thus the array of the grains is also relatively regular.

The effects of mechanical vibration on the remanufacturing layer are all achieved via the influence on molten pools, since the welding-seam molten pool is the most fundamental forming unit of the remanufacturing layer. The research of Ref. [30] pointed out that the macro effect of mechanical vibration on molten pools is implemented through the following two aspects: the first one is that the liquid metal also implements a forced vibration through the interaction between the walls of the molten pool and the metal in the molten pool when the welding piece is subjected to a forced vibration. The second one is that the arcing pressure varies since the length of the welding arc varies due to the vibration of the welding piece. It is equivalent to a periodic exciting force being exerted on the liquid metal surface of the molten pool and disturbing the liquid metal. From the point of view of the solidification theory, the effect of vibration on the remanufacturing microstructure fundamentally influences the nucleation and growth behavior of crystals during the metal solidification.

During the process of metal solidification, with the decrease of temperature, embryo crystallisties begin to form firstly. However, only the embryo crystallisties with a size equal to or bigger than the critical crystal nucleus radius can exist in a stable manner and spontaneously develop and become crystal grains at last. The critical crystal nucleus radius r_k can be figured out according to the following equation:

$$r_k = \frac{2\sigma T_{\mathrm{m}}}{L_{\mathrm{m}}\Delta T} \tag{2}$$

where σ is the surface energy per unit area, T_{m} is the theoretical crystallization temperature, L_{m} is the latent heat of fusion, and ΔT is the undercooling degree. It can be seen from Eq.(2) that the critical crystal nucleus radius r_k is inversely proportional to the undercooling degree ΔT, namely,

the greater the value of undercooling degree ΔT, the smaller the critical crystal nucleus radius. The Ref.[31] shows that during the process of metal solidification, the Reynolds number of liquid metal will be gradually increased due to the implementation of vibration and the increase of the vibrational frequency. The larger the Reynolds number, the higher the flow turbulence extent of the liquid metal and the higher the heat transfer efficiency. This means that the undercooling degree of the whole molten pool is enlarged so that the nucleation rate is increased. In this experiment, a larger vibration speed means a higher vibrational frequency, and the undercooling degree of the molten pool under the corresponding conditions is larger so that the nucleation rate is relatively higher.

Meanwhile, a mechanical vibration will cause the amplitude of the liquid metal's energy fluctuation to change and to enlarge. The periodic number of energy fluctuation per unit length is also increased [32]. After the stable nucleation occurred, the vibration can increase the periodic number of energy fluctuation per unit length. Consequently the attachment and escape time of atoms on the crystal surface will increase. However, since the crystal nucleus is in a stable and growing stage, the grain grows gradually. This is because, generally, the attachment time of atoms is greater than escape time of atoms. In general, the higher the nucleation rate, the smaller the growth rate and the finer the grains[32, 33]. Thus, the effect of refining grains can be obtained by imposing the vibration with a certain rotation speed in the remanufacturing process of FV520B stainless steel by MAG surfacing deposition technology, so that the width of martensite lath can be narrowed. However, the research of Ref.[34] points out that the vibration will also correspondingly increase the kinetic energy of atoms and each nucleation particle and finally causes a certain heat effect. The higher the vibrational frequency, the more significant the generated heat effect. When the heat effect reaches a certain level, the growing time of the grains will be delayed and the grains will be coarsened. Therefore, the width of martensite lath in the remanufacturing layer has a widening trend in the end.

The research displayed in Ref.[35-37] points out that during the process of metal solidification, a liquid phase flow can have a flushing effect and a mechanical breaking action on the grains and thus causes the crystal grains to break. The application of mechanical vibration can have a stirring action on the molten metal and speed up the flow of molten metal. The higher the vibrational frequency, the stronger this kind of stirring and broken function. This is the main reason why the fragments of martensite laths appeared in the remanufacturing TEM images shown in Fig.4. Meanwhile, due to the addition of vibration, the heat flow during the solidification process of molten pool is more turbulent and the crystallization behavior is more complex, and then the probability of obtaining twinning formation is increased, as shown in Fig.6.

As mentioned above, the solidification forming of surfacing material during the remanufacturing of FV520B stainless steel by MAG surfacing deposition technology is a rapid cooling non-equilibrium crystallization process. Therefore, the lattice distortion is caused by a large number of defects, such as vacancies, dislocations and foreign atoms. After applying a vibration, from the microscopic view, certain kinetic energies are imposed to each crystal lattice. Once the sum of imposed energy values and the microstructure original energy value are enough to overcome the surrounding well potential of the microstructure (the binding force for equilibrium restoration), plastic deformation will occur within the micro-zone, so that the distorted crystal lattices can slowly recover and reach the equilibrium state. Thus, a mechanical vibration can eliminate the lattice distortion to some extent, and reduces the angle of Bragg diffraction peak position in the remanufacturing layer, and then the FWHM become narrower. The kinetic energy obtained by each crystal lattice will be different when the vibration speeds are different. Thus, under the conditions of different vibration speeds, the angle offsets of the Bragg diffraction peak position and the narrowing extent of FWHM in the remanufacturing layer are different.

The higher the vibration speed, the larger the kinetic energy that can be obtained by each crystal lattice. However, the over-high energy may generate an excessive plastic deformation, which will cause a new lattice distortion during the original lattice distortion elimination. Therefore, after the vibration reaches a certain rotation speed of $f \geq 3000$ r/min, a rebound phenomenon of the angle offset of Bragg diffraction peak position and the FWHM narrowing appear with the constant increase of the vibration speed. Previous research[38] points out that when the vibration method is adopted to relieve the stress of a workpiece, the vibrational frequency is normally selected in front of the resonance peak, namely, the sub-resonance region of the workpiece (the vibrational frequency is 1/3~2/3 of the resonance frequency) achieves the optimum effect, which has a good consistency with the most significant effect of vibration on the remanufacturing microstructure when the rotation speed reaches f=3000 r/min.

In addition, during the solidification forming process of remanufacturing deposition material, the dislocation density and tangle extent within each crystal plane are different. Thus, after a vibration is imposed and when the lattice distortion is restored, the resistance of the lattice array to the dislocation movement of each crystal plane is different, so that the narrowing extent of the Bragg diffraction peak in each crystal plane is also different at the same vibration speed.

The preferred orientation of the crystal plane is formed by the grain rotation under the function of applied stress. When the state of applied stress is different, the rotating mode of grains will be different so that the generated preferred orientation will be changed as well. This kind of preferred orientation results in different levels of anisotropies in the materials, and the strengths along different directions are variable[39]. Since the direction of mechanical vibration is definite, the orientation of the impact force on the remanufacturing layer is also determined. However, the growth orientation of each crystal grain is different, and the dislocation density and tangle extent within each crystal plane are different as well. Furthermore, the preferred orientation variation of each crystal plane is variable at the same vibration speed. In general, the application of vibration can enhance the preferred orientation of crystals during the growing process.

3 Conclusions

1) Due to the remanufacturing characteristics of surfacing deposition technology, the remanufacturing microstructure of FV520B stainless steel using MAG surfacing deposition technology corresponds to a rapid cooling non-equilibrium crystallization, which is lath martensite+carbide precipitation hardening phases of NbC, Mo_2C, M_7C_3 and $M_{23}C_6$. The microstructure appears as a periodical variation rule and has a certain self-similar fractal characteristic.

2) The disturbance effect of vibration to the molten pool and its kinetic energy can improve the nucleation rate of the welding pool to a certain degree, narrow the width of martensite lath and have a broken effect on the martensite lath. However, with the continuous increase of the vibration speed, the width of martensite lath decreases first and then increases. Meanwhile, the incorporation of vibration can complicate the crystallization behavior in the welding pool and increase the probability of twin formation.

3) The kinetic energy produced by the vibration can change the extent of lattice distortion and has an effect on the preferred orientation of each crystal plane. With the continuous increase of the vibration speed, the extent of the lattice distortion first weakens and then increases. The preferred orientation of crystal plane (110) is first enhanced and then weakens with the continuous increase of the vibration speed. During the remanufacturing process, the addition of vibration in the sub-resonance region has an optimum effect on eliminating the lattice distortion, enhancing the preferred orientation of crystal plane (110) and refining the crystal grains.

References

1 Li Rongpeng. *The Investigation of Casting Martensite Precipitation Hardening Stainless Steel Impeller Materials and Technics*[D]. Shenyang: Shenyang University of Technology, 2006 (in Chinese)

2 Ren Weibin, Dong Shiyun, Xu Binshi *et al. Materials Engineering*[J], 2015, 43(1): 6 (in Chinese)

3 Wang J L, Zhang Y L, Liu S J *et al. International Journal of Fatigue*[J], 2016, 87: 203

4 Liu C, Liu S J, Gao S B *et al*. *Engineering Failure Analysis*[J], 2016, 66: 177

5 Niu Jing, Dong Junming, Xue Jin. *Chinese Journal of Mechanical Engineering*[J], 2007, 43(12): 78 (in Chinese)

6 Chen Jinming, Huo Haiyan, Hu Changguo. *Compressor, Blower and Fan Technology*[J], 2014(5): 58 (in Chinese)

7 Li Hongkun, Zhao Pengshi, Li Jingzhong *et al. Journal of Vibration, Measurement & Diagnosis*[J], 2015, 35(4): 722 (in Chinese)

8 Zhao Lei, Hu Changyuo, Wu Daoxia *et al. Machine Tool & Hydraulics*[J], 2013, 41(1): 54 (in Chinese)

9 Zhou Qianqing, Zhai Yuchun. *Acta Metallurgica Sinica*[J], 2009, 45(10): 1249 (in Chinese)

10 Xu Wenbo, Shi Wei, Zhang Xin. *Transactions of Materials and Heat Treatment*[J], 2013, 34(11): 139 (in Chinese)

11 Fan Junling, Guo Xinglin, Wu Chengwei *et al*. *Chinese Journal of Materials Research*[J], 2012, 26(1): 61 (in Chinese)

12 Xiao Furen. *Transactions of Metal Heat Treatment*[J], 1999, 20(4): 35 (in Chinese)

13 Fan Junling, Guo Xinglin, Wu Chengwei. *Journal of Materials Engineering*[J], 2013, 41(7): 1 (in Chinese)

14 Han Zengfu, Zhang Feixiong. *General Machinery*[J], 2003, 7: 31

15 Zhang Min, Li Yan, Li Jihong *et al. China Mechanical Engineering*[J], 2011, 22(22): 2749 (in Chinese)

16 Niu Jing, Dong Jinming, Xue Jin *et al. Transactions of the China Welding Institution*[J], 2006, 27(12): 101 (in Chinese)

17 Zhang Min, Liu Mingzhi, Zhang Ming *et al. Journal of Materials Engineering*[J], 2016, 44(3): 40 (in Chinese)

18 Hao Shengzhi, Zhao Limin, Wang Huihui *et al. Chinese Journal of Vacuum Science and Technology*[J], 2015, 35(12): 1519 (in Chinese)

19 Bao Cuimin, Zhuang Chunyu, Chen Rui *et al*. *Materials Protection*[J], 2015, 48(6): 7 (in Chinese)

20 Li Fashuang, Li Fangyi, Jia Xiujie *et al. Tool Technology*[J], 2015, 49(10): 55 (in Chinese)

21 Liu Jian. *Study of GMAW Surface Forming with Non-support Structure Based on Arc Weld Robot*[D]. Beijing: Academy of Armored Forces Engineering, 2011 (in Chinese)

22 Zhu Hua, Ji Cuicui. *Theory and Application of Fractal*[M]. Beijing: Science Press, 2011 (in Chinese)

23 Liu Jian, Zhu Sheng, Yang Junwei *et al. Journal of Academy of Armored Force Engineering*[J], 2014, 28(3): 93 (in Chinese)

24 Korchef A, Champion Y, Njah N. *Journal of Alloys and Compounds*[J], 2007, 427(1-2): 176
25 Su Yunhai, Ma Dahai, Lin Jinliang *et al. Transactions of the China Welding Institution*[J], 2014, 35(9): 49 (in Chinese)
26 Chang Xuejun, Wang Wenli, Xu Ruichao *et al. Hot Working Technology*[J], 2015,44 (3): 104 (in Chinese)
27 Wang Leyou, Wu Wenxiang, Ma Ke *et al*. *Materials and Technology*[J], 2010, 18(6): 838 (in Chinese)
28 Yang Jiaoxian. *Physical Basis for Plastic Deformation of Metals*[M]. Beijing: Metallurgical Industry Press, 1987 (in Chinese)
29 Li Zhanming. *Research on Ultrasonic Strengthening Techniques and Mechanism of Aluminum Alloy Welding Joint*[D]. Beijing: Academy of Armored Forces Engineering, 2010 (in Chinese)
30 Guan Jianjun, Song Tianmin, Zhang Guofu *et al. Journal of Fushun Petroleum Institute*[J], 2001, 21(4): 51 (in Chinese)
31 Wang Chao, Zhang Hui, Zhu Xinhun *et al*. *Iron and Steel*[J], 2010, 45(10): 37 (in Chinese)
32 Hu Gengxiang, Qian Miaogen. *Metallography*[M]. Shanghai: Shanghai Science and Technology Press, 1982 (in Chinese)
33 Lu Qinghua, Chen Ligong, Ni Chunzhen. *Journal of China Mechanical Engineering*[J], 2007, 18(20): 2497 (in Chinese)
34 Jiang Ripeng, Li Xiaoqian, Hu Shicheng *et al*. *Materials for Mechanical Engineering*[J], 2008, 32(10): 14 (in Chinese)
35 Wu Xiaofeng, Zhang Guangan, Zhou Qi. *Foundry*[J], 2009, 58(10): 1002 (in Chinese)
36 Yang Zhijie, Cang Daqiang, Li Yu. *Foundry*[J], 2011, 60(1): 77 (in Chinese)
37 Dong Zhanren, Kong Fange, Liu Limin. *Welding & Jointing*[J], 1999(7): 21 (in Chinese)
38 Zhao Xianhua. *Principle and Application of Vibration Aging*[M]. Jinan: Shandong Huawin Electrical Technology Co, Ltd, 2012 (in Chinese)
39 Gao Bo, Sun Shuchen, Zhao Tiejun *et al. Chinese Journal of Rare Metals*[J], 2007, 31(3): 293 (in Chinese)

振动对 FV520B 不锈钢 MAG 堆焊再制造成形组织结构的影响

柳 建[1]，朱 胜[2]，蔡志海[1]，张 平[1]，刘 军[1]，秦 航[1]，仝永刚[1]
(1. 装甲兵工程学院 机械产品再制造国家工程研究中心，北京 100072)
(2. 装甲兵工程学院 装备再制造技术国防科技重点实验室，北京 100072)

摘 要：采用堆焊熔敷成形技术进行了FV520B沉淀硬化不锈钢再制造实验，在此基础上，对FV520B不锈钢熔化极活性气体保护电弧焊 (metal active gas arc welding, MAG)堆焊再制造成形组织特点进行了分析，并研究了机械振动对再制造成形组织的影响。结果显示：FV520B不锈钢MAG堆焊再制造成形组织由马氏体+碳化物沉淀硬化相组成，且沿成形高度方向组织呈周期性变化特点，具有一定的自相似分形特性；振动会一定程度上增大孪晶形成几率，对马氏体板条具有破断作用，且马氏体板条宽度随振动转速的不断增大呈先减小后增加趋势；受振动的影响，晶格畸变和各晶面择优取向性都将发生变化，但不同晶面变化规律不同；振动的加入使得 (110) 晶面和 (211) 晶面的Bragg衍射峰峰位向低衍射角方向发生偏移，且随振动转速的不断增大，偏移量呈先增大后减小趋势，（110）晶面衍射峰半高宽呈先减小后增大趋势，其晶面择优取向 (TC) 性则呈现先增强后减弱趋势；在0到共振转速区间内 (211) 晶面衍射峰半高宽随振动转速的不断增大呈先减小后增大趋势，当振动转速大于共振转速时又呈减小趋势，但其晶面择优取向 (TC) 性则随振动转速的增大呈现持续增强趋势；总体上，亚共振频率振动（振动转速f=3000 r/min）对FV520B不锈钢MAG堆焊再制造成形组织结构的影响最显著。

关键词：FV520B 沉淀硬化不锈钢；再制造；MAG 堆焊；振动；组织结构

作者简介：柳 建，男，1982 年生，博士，装甲兵工程学院机械产品再制造国家工程研究中心，北京 100072，电话：010-66717416，E-mail: 550123310@qq.com